


# Biopreservation of living tissue engineered nerve grafts

Journal of Tissue Engineering  
Volume 12: 1–14  
© The Author(s) 2021  
Article reuse guidelines:  
sagepub.com/journals-permissions  
DOI: 10.1177/20417314211032488  
journals.sagepub.com/home/tej



Robert B Shultz<sup>1,2,3,5</sup> , Kritika S Katiyar<sup>1,2,5</sup>,  
Franco A Laimo<sup>1,2</sup>, Justin C Burrell<sup>1,2,4</sup>, Kevin D Browne<sup>1,2</sup>,  
Zarina S Ali<sup>2,6</sup> and Daniel K Cullen<sup>1,2,4,5</sup>

## Abstract

Tissue engineered nerve grafts (TENGs) built from living neurons and aligned axon tracts offer a revolutionary new approach as “living scaffolds” to bridge major peripheral nerve defects. Clinical application, however, necessitates sufficient shelf-life to allow for shipping from manufacturing facility to clinic as well as storage until use. Here, hypothermic storage in commercially available hibernation media is explored as a potential biopreservation strategy for TENGs. After up to 28 days of refrigeration at 4°C, TENGs maintain viability and structure *in vitro*. Following transplantation into 1 cm rat sciatic defects, biopreserved TENGs routinely survive and persist for at least 2 weeks and recapitulate pro-regenerative mechanisms of fresh TENGs, including the ability to recruit regenerating host tissue into the graft and extend neurites beyond the margins of the graft. The protocols and timelines established here serve as important foundational work for the manufacturing, storage, and translation of other neuron-based tissue engineered therapeutics.

## Keywords

Tissue engineered nerve graft, tissue engineered medical product, biopreservation, hypothermic storage, living scaffold

Date received: 23 May 2021; accepted: 24 June 2021

## Introduction

Tissue engineering has the potential to transform patient care by providing therapies that can address a host of diseases and injuries affecting various organs. Tissue engineered medical products (TEMPs) strive to restore lost function by replacing and/or reconstructing damaged tissue and organs. To date, translational development of TEMP has largely focused on identifying clinically viable cell sources and optimizing tissue culture and/or bioreactor conditions. Effective biopreservation of the final product, however, is critical for translation as it allows for shipment from manufacturing facility to clinic and storage prior to use.<sup>1</sup> The goal of biopreservation is to achieve a functionally consistent end-product; for living cell-based TEMP, this requires careful maintenance of multiple interconnected processes including cellular viability and phenotype, surrounding matrix integrity, and overall tissue architecture and potency. Several biopreservation strategies have been proposed including hypothermic storage, cryopreservation, vitrification, and desiccation/dry storage.<sup>2</sup> Among these, hypothermic storage has been most widely adopted for clinical use, as most protocols do not require the use of toxic cryoprotective agents or

specialized equipment beyond standard refrigerators. To date, hypothermic preservation strategies have been implemented to extend shelf lives of cells, tissues and organs such as red blood cells,<sup>3</sup> hepatocytes,<sup>4</sup> mesenchymal stromal cells,<sup>5</sup> adipose stem cells,<sup>6</sup> cornea,<sup>7</sup> native and engineered skin,<sup>8,9</sup> nerve allografts,<sup>10</sup> engineered bone,<sup>11</sup> and solid organs.<sup>12</sup> Hypothermic storage exploits the temperature dependence of nearly all biochemical

<sup>1</sup>Center for Neurotrauma, Neurodegeneration & Restoration, Corporal Michael J. Crescenzo Veterans Affairs Medical Center, Philadelphia, PA, USA

<sup>2</sup>Center for Brain Injury and Repair, Department of Neurosurgery, University of Pennsylvania, Philadelphia, PA, USA

<sup>3</sup>Department of Chemistry and Chemical Biology, School of Arts and Sciences, Rutgers University, Piscataway, NJ, USA

<sup>4</sup>Department of Bioengineering, School of Engineering and Applied Science, University of Pennsylvania, Philadelphia, PA, USA

<sup>5</sup>Axonova Medical, LLC, Philadelphia, PA, USA

<sup>6</sup>Penn Nerve Center, University of Pennsylvania, Philadelphia, PA, USA

### Corresponding author:

D. Kacy Cullen, Center for Neurotrauma, Neurodegeneration & Restoration, Corporal Michael J. Crescenzo Veterans Affairs Medical Center, Philadelphia, PA 19104-4594, USA.

Email: dkacy@pennteam.upenn.edu



Creative Commons Non Commercial CC BY-NC: This article is distributed under the terms of the Creative Commons

Attribution-NonCommercial 4.0 License (<https://creativecommons.org/licenses/by-nc/4.0/>) which permits non-commercial use, reproduction and distribution of the work without further permission provided the original work is attributed as specified on the SAGE and Open Access pages (<https://us.sagepub.com/en-us/nam/open-access-at-sage>).

reaction rates to effectively slow biological time.<sup>13</sup> At reduced temperatures, the rates of maturation, metabolism, and any active degenerative processes are substantially delayed, effectively preserving tissue viability and function.

In the current study, we have adapted hypothermic preservation techniques to successfully preserve and store tissue engineered nerve grafts (TENGs) used to repair critical defects in peripheral nerves. The current gold standard treatments for long gap nerve injuries are autologous nerve grafts (autografts) that require sacrificial harvest of healthy nerve to repair damaged nerve, deliberately creating a second injury—and associated functional loss—to surgically repair the initial injury. Even following state-of-the-art repair, however, clinical outcomes following nerve autografting frequently remain poor.<sup>14</sup> For shorter gaps, nerve guidance conduits or acellular nerve allografts can be utilized, although actual clinical use of these products is limited almost entirely to the repair of short sensory nerve defects in distal locations such as the hand.<sup>14</sup>

TENGs offer a transformative approach to repairing currently untreatable injuries in peripheral nerves. TENGs are comprised of aligned, living axon bundles spanning neuronal aggregates and can be grown to clinically relevant lengths (5–10 cm) from translationally-viable tissue sources in our custom-built mechanobioreactors.<sup>15,16</sup> Upon transplantation into nerve defects, the engineered tissue has been shown to recruit host Schwann cells (SCs) and axons into the defect.<sup>15,17</sup> At the same time, TENG neurons have been shown to extend axons into the distal nerve stump where they may interact with host SCs and preserve the regenerative capacity of distal structures.<sup>18</sup> Finally, TENGs have also been shown to exert protective effects proximally on host neuron populations.<sup>19</sup> By targeting multiple synergistic pathways, TENGs may provide a revolutionary approach to peripheral nerve reconstruction. Indeed, in both rodents<sup>15,17–19</sup> and swine,<sup>20</sup> TENG transplantation has been shown to dramatically improve regeneration of host nerve as compared to nerve guidance conduits, performing at least as well as autografts. Clinical application of this strategy, however, necessitates shelf life, a major barrier to translation for all living TEMPs.

In this study, a protocol was established to allow for up to 4 weeks of TENG storage without the use of specialized equipment or hazardous reagents. The effect of biopreservation on TENG neuron/axon viability, cytoskeletal constituents/integrity, and interactions with host cells were evaluated using both *in vitro* and *in vivo* methods (Figure 1). In addition to advancing TENG translation, these findings can inform biopreservation efforts for the broader tissue engineering community.

## Materials and methods

All procedures were approved by the Institutional Animal Care and Use Committees at the University of Pennsylvania

and the Corporal Michael J. Crescenz Veterans Affairs Medical Center and adhered to the guidelines set forth in the NIH Public Health Service Policy on Humane Care and Use of Laboratory Animals.

### Dorsal root ganglia harvest

Dorsal root ganglia (DRG) neurons were harvested as previously described.<sup>17,19</sup> Briefly, intact spinal cords were extracted from embryonic day 16 Sprague Dawley pups, and whole DRG were plucked from the spinal cord and placed in cold Leibovitz-15 (L-15) medium (ThermoFisher). Once the desired number of DRGs were harvested, they were rinsed twice in plating media consisting of Neurobasal<sup>®</sup> medium (ThermoFisher) supplemented with 2% B-27 (ThermoFisher, 500  $\mu$ M L-glutamine, 1% FBS (Atlanta Biologicals), 2.5 mg/mL glucose (Sigma), 20 ng/mL 2.5S nerve growth factor (BD Biosciences), 20 mM 5FdU (Sigma), and 20 mM uridine (Sigma). Sex of the pups was not determined.

### TENG fabrication and biopreservation

Explants were plated into custom-built mechanobioreactors to induce stretch growth, as described previously (Figure 1).<sup>17</sup> Briefly, the mechanobioreactors contained two adjoining membranes of 33C Aclar (SPI supplies) treated with 20  $\mu$ g/mL poly-D-lysine (BD Biosciences) and 20  $\mu$ g/mL laminin (BD Biosciences). One of these membranes, denoted the “towing membrane,” could be precisely moved by a stepper motor. The DRG explants were plated in two populations on either side of the membrane interface to allow formation of axonal networks between these two populations over 5 days *in vitro*. To allow for *in vivo* identification, a subset of cultures were transduced to express GFP with an AAV viral vector as previously described (AAV2/1.hSynapsin.EGFP.WPRE.bGH, UPenn Vector Core).<sup>17</sup> A stepper motor system was then engaged to separate the populations in micron-size increments until the TENGs reached 1 cm. Stretched cultures were encapsulated in an extracellular matrix (ECM) comprised of 3.0 mg/mL rat-tail collagen type I (BD Biosciences) supplemented with 2.5S nerve growth factor (BD Biosciences). Once encapsulated, the TENGs were transferred to a petri dish containing 5 mL of biopreservation media (Hibernate-E supplemented with B27, Penicillin/Streptomycin, and Glutamax, all from Thermo Fisher Scientific) and stored at 4°C until the terminal time point (up to 28 days). A total of 47 TENGs were fabricated for all studies; 36 were used for *in vitro* testing, and 11 were transplanted *in vivo*.

### Lactate dehydrogenase assay

To quantify lactate dehydrogenase (LDH) release, 100  $\mu$ L of biopreservation media was sampled without replacement

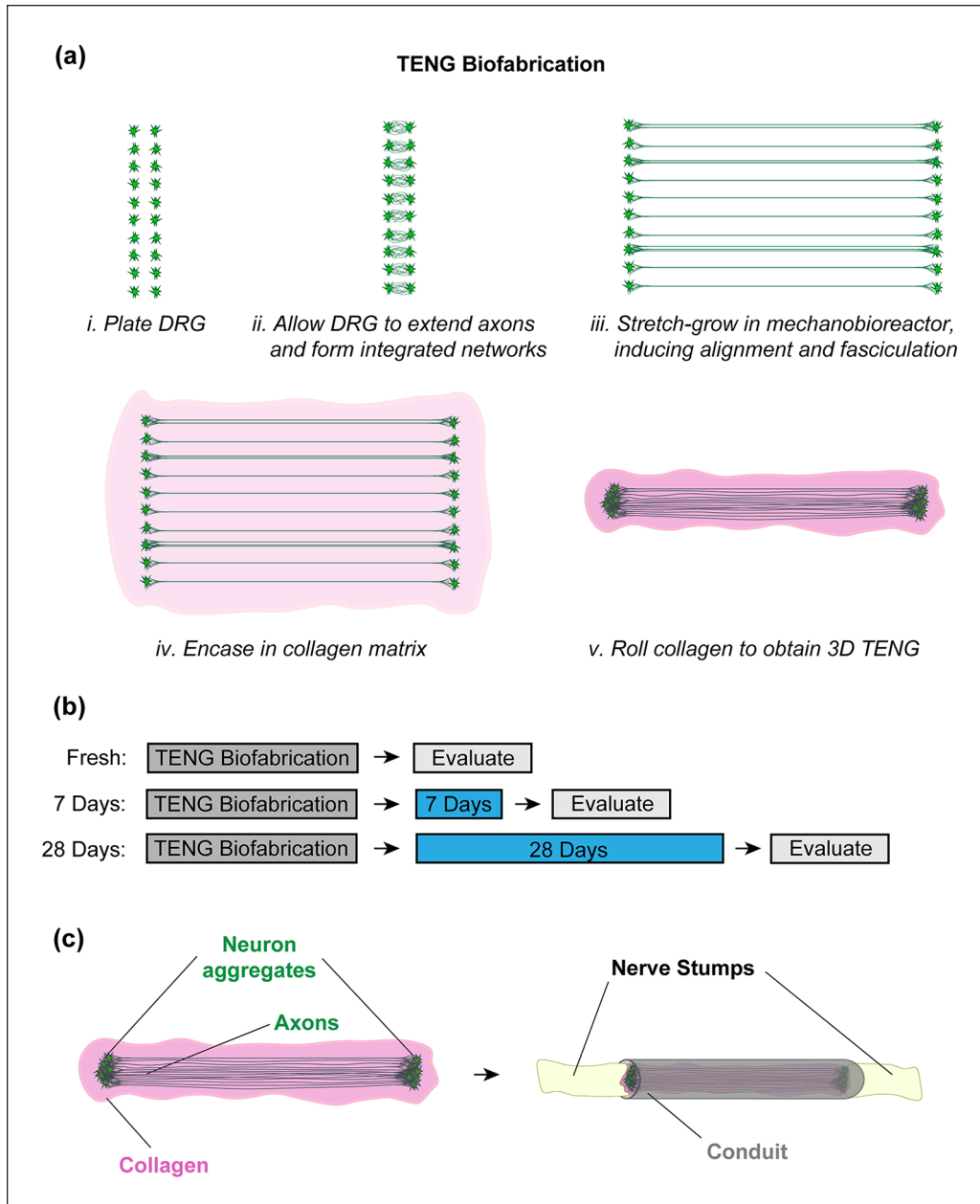


**Figure 1.** Conceptual illustration of study: (a) overview of TENG biofabrication process, (b) explanation of group names; TENGs were evaluated using in vitro and in vivo methods after 0, 7, or 28 days of biopreservation, and (c) schematic illustrating a TENG comprised of collagen-encapsulated stretch grown axons before and after transplantation into a 1 cm sciatic nerve defect.

after 24h and weekly thereafter from TENGs ( $n=6$ ) biopreserved for 28 days. Over the entire duration of biopreservation (up to 28 days), no media changes were performed. To determine maximal LDH release indicative of total TENG failure, a subset of TENGs ( $n=6$ ) were crushed using a glass homogenizer and left to release LDH into the surrounding media for 24 h prior to sample collection. All samples were immediately frozen and stored at  $-80^{\circ}\text{C}$  until use, when LDH enzyme activity levels were quantified with an LDH assay kit (Abcam). To determine LDH activity, samples are incubated with substrate, which is converted into NADH, as well as probe, which becomes fluorescent upon binding to NADH. As product accumulates, fluorescent signal grows in

intensity. Samples were mixed with substrate and probe on ice and then transferred to a microplate spectrophotometer pre-heated to  $37^{\circ}\text{C}$ . Fluorescent measurements (535/587 nm excitation/emission) were taken every 5 min using a microplate spectrophotometer (BioTek), and enzyme activity calculated from the data according to manufacturer's instructions.

#### *Live/dead labeling and immunocytochemistry of biopreserved TENGs in vitro*

To label live and dead cells, TENGs were incubated for 30 min at  $37^{\circ}\text{C}$  in DPBS containing Calcein AM and ethidium homodimer according to manufacturer's instructions

(Thermo Fisher Scientific). Upon uptake into living cells, nonfluorescent cell-permeable Calcein AM is converted to green-fluorescent, membrane-impermeable calcein by intracellular esterases. Because dead cells lack esterase activity, only living cells are brightly labeled green. Ethidium homodimer is a weakly fluorescent cell-impermeant dye that exhibits bright red fluorescence upon intercalation with DNA base pairs. Because ethidium homodimer can only enter the nuclei of cells with damaged plasma and nuclear membranes, only dead cells are brightly labeled red. A total of five TENGs were subjected to live/dead staining ( $n=1$  fresh and  $n=4$  28 day-biopreserved TENGs).

For immunocytochemistry, TENGs were fixed with 4% paraformaldehyde either immediately after encapsulation ( $n=3$ ) or following 7 or 28 days of biopreservation ( $n=3$  each). Fixed TENGs were then blocked and permeabilized in 1x PBS containing 0.1% Triton X-100 (Sigma) and 4% normal horse serum (NHS) for 1 h and stained with primary antibodies overnight at 4°C. Primary antibodies raised against beta-III tubulin (Tuj1; Sigma), neurofilament 200 (NF-200; Sigma), and neuronal nuclei (NeuN; Millipore) were diluted 1:500 in PBS containing 4% NHS. After extensive rinsing to remove unbound antibodies, TENGs were incubated in Alexafluor-conjugated secondary antibody solutions (ThermoFisher; 1:500 in PBS) for 2 h at room temperature. Nuclei were counterstained with DAPI (ThermoFisher; 1:2000 in PBS) for 15 min and extensively washed prior to imaging. All antibodies used have been validated in our lab for use with TENGs and rodent tissue.<sup>17,19,21,22</sup>

### Peripheral nerve surgery and repair

Rat sciatic nerve lesions (1 cm) were created and surgically repaired with TENGs as previously described.<sup>17</sup> Briefly, adult male Sprague-Dawley rats (Charles River) were anesthetized with 2.5% isoflurane, and the left sciatic nerve exposed. A 0.9 cm segment was excised and replaced with a TENG housed within a 1.2 cm long clinically available crosslinked collagen nerve wrap (Neuromend, Stryker). After placing the TENG in the wrap, 8-0 sutures were used to close the wrap and form a conduit. Nerve stumps were fixed via epineurial suture at a depth of 1 mm into the conduit at each end, creating a gap length of 1.0 cm. The wound site was then closed in layers with 4-0 sutures and staples. Animals received TENGs either freshly prepared ( $n=3$ ) or biopreserved for 7 or 28 days before transplantation ( $n=2$  and  $n=6$ , respectively).

### Tissue processing and staining

At 2 weeks post-implant, animals were euthanized via CO<sub>2</sub> inhalation followed by decapitation. The sciatic nerve was re-exposed, and a length of nerve including the graft region plus 3–5 mm of proximal and distal stump was removed and post-fixed in ice cold 4% paraformaldehyde for 48 h.

After cryoprotecting in 30% sucrose for 48 h or until fully saturated, the tissue was embedded in OCT (Tissue Tek) and frozen at -80°C. 20 μm longitudinal sections were then taken with a Microm HM 550 cryotome (ThermoFisher) and collected on Superfrost slides (Fisher). All slides were visually examined for the presence of TENG-derived tissue. A subset of sections spanning the entire nerve at approximately 160 μm intervals were labeled with the following primary antibodies diluted 1:500 in PBS containing 0.3% Triton X-100 and 4% NHS: SMI31+32 (phosphorylated and nonphosphorylated neurofilaments, BioLegend); S100 (Invitrogen); and GFP (Abcam). After extensive rinsing, sections were then incubated in Alexafluor-conjugated secondary antibody solutions (ThermoFisher; 1:500 in PBS) for 2 h at room temperature. To preserve fluorescent signal, stained samples were treated with Fluormount-G (ThermoFisher) prior to coverslipping.

### Microscopy and image analysis

Phase-contrast images of TENGs were captured using a Nikon Eclipse Ti-S inverted microscope. Fluorescent images of TENGs or tissue sections were taken with either a Keyence BZ-X810 fluorescent microscope or a Nikon A1RSI Laser Scanning Confocal microscope. When capturing images to be used for fluorescence intensity quantification, acquisition parameters including magnification, laser power, pinhole size, high voltage gain, and resolution were kept consistent across samples to allow for accurate comparison. All image analysis was performed with ImageJ software. For quantification of fascicle number, the number of fascicles was counted from an area that was equidistant from the towing membrane from images of a fresh, pre-encapsulated construct ( $n=5$ ; phase/contrast) and the corresponding TENG after biopreservation for 7 or 28 days ( $n=2$  and 3, respectively; fluorescent). The percent of fascicles remaining after 7 and 28 days compared to the pre-encapsulated construct was calculated. Additionally, the diameter of each fascicle/axon was measured and averaged to give a representative fascicle diameter for each TENG prior to encapsulation (i.e. fresh TENG) as well as following 7 and 28 days of biopreservation. For quantification of fluorescence intensity, the average intensity of pixels above a background threshold value was calculated. For quantification of NeuN+ nuclear area, the number of pixels above background threshold on the NeuN channel (far red) was divided by the number of pixels above background threshold on the DAPI channel (blue). Thresholds were chosen to remove background signal, which would dramatically influence average intensity and area percentages, and were kept consistent across all images. For evaluation of overall TENG health/architecture, TENG-derived DRG health, and SC interaction, scores were assigned according to semi-quantitative ordinal scales described in detail in Supplemental Figure 1.



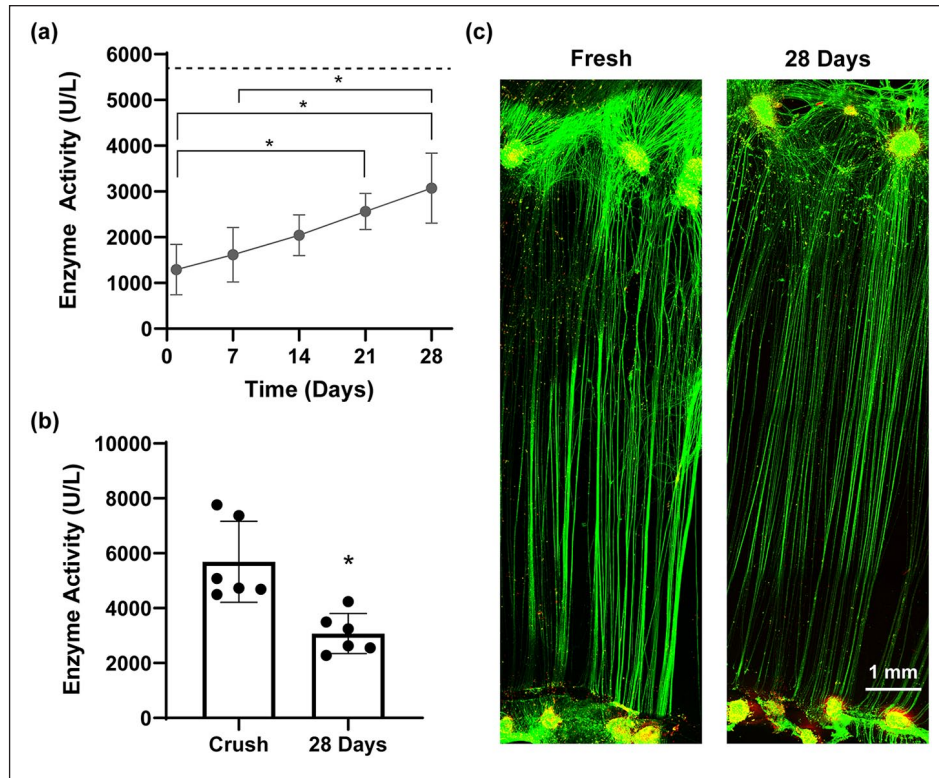


**Figure 2.** TENGs survive biopreservation for up to 28 days: (a) LDH enzyme activity, an indicator of compromised cell membranes, increases over time but does not reach levels indicative of total TENG failure (dashed line denotes average LDH released by a crushed TENG), (b) after 28 days of biopreservation, LDH enzyme activity remains significantly lower than following crush injury ( $p < 0.05$ ), and (c) fresh and biopreserved TENG neurons and axons exhibit similar live/dead (green/red) staining with neurons and long axons robustly retaining calcein following calcein-AM live staining.

### Statistical analysis

All statistical analysis was performed using GraphPad Prism 8 software (GraphPad Software, Inc). Data are graphically represented as mean  $\pm$  standard deviation error bars. For comparisons involving multiple groups, nonparametric Kruskal-Wallis tests were employed. For repeated measures, a nonparametric Friedman test was used instead. In both cases, pairwise comparisons were tested with Dunn post-hoc tests. For direct comparisons between two groups, a Mann-Whitney  $U$ -test was used. For all tests, significance was evaluated using 0.05 as the cutoff  $p$ -value.

## Results

### TENGs survive biopreservation for up to 28 days

To assess the effect of biopreservation on construct survival, collagen-encased stretch-grown cultures were placed in petri dishes containing 5 mL biopreservation media and transferred to 4°C for up to 28 days. Media was sampled after 24 h and weekly thereafter and tested for the presence of lactate dehydrogenase (LDH). In healthy cells, LDH is sequestered inside the plasma membrane; LDH

release into the media is thus indicative of membrane breakdown and degeneration.

Across 28 days of biopreservation, media collected from TENGs exhibited a steady increase in LDH activity, indicating accumulating LDH enzyme in the extracellular space (Figure 2(a)). After 21 days of biopreservation, enzyme activity was statistically higher than after 1 day. By 28 days, enzyme activity was statistically higher than after either 1 or 7 days. Even at 28 days, however, enzyme activity only reached about half of the levels observed following TENG crush (Figure 2(b)). In addition, collagen-encased TENGs either freshly prepared or biopreserved for 28 days exhibited robust green fluorescent signal indicative of calcein retention in both neuronal somas and axon tracts (Figure 2(c); green). Fresh and biopreserved cultures also contained similar levels of ethidium homodimer-labelled dead cells typical of DRG explant cultures (Figure 2(c), red).

### Biopreserved TENGs maintain fascicular architecture

The robust calcein uptake into axon tracts observed in Figure 2(c) suggested structural TENG maintenance across

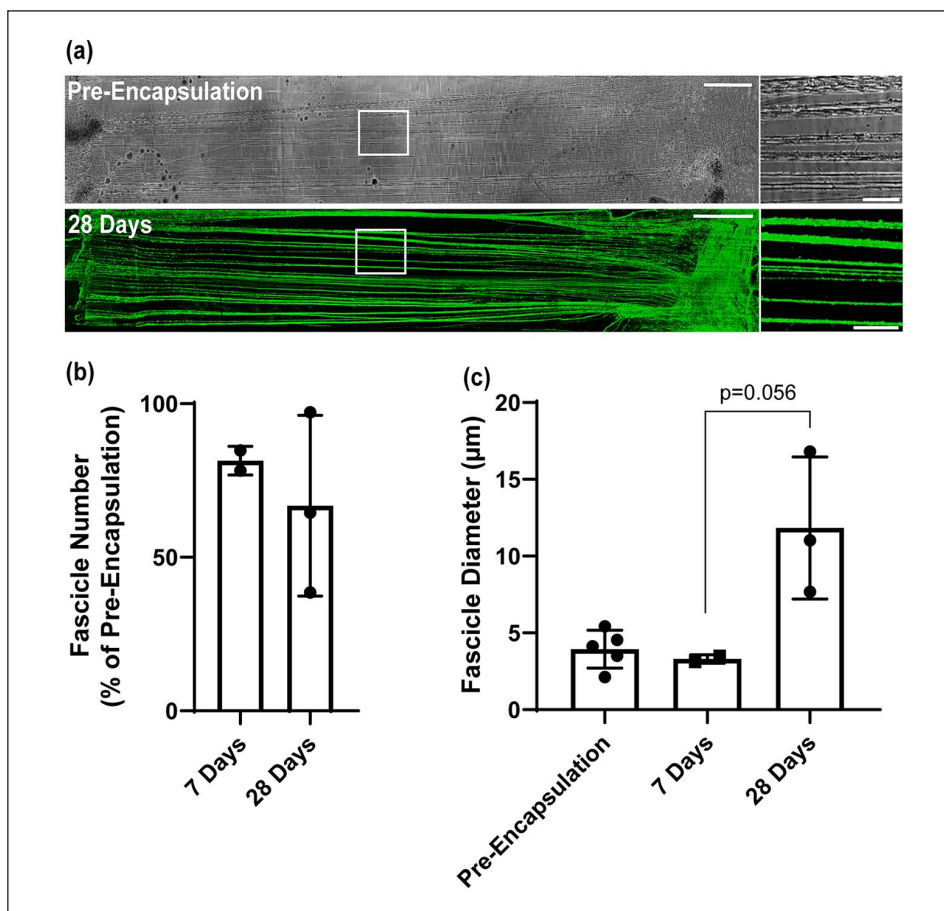


**Figure 3.** TENG fascicular architecture across 28 days of biopreservation: (a) phase-contrast image of stretch-grown axons prior to collagen encapsulation, and TuJ1 + TENG after hibernation for 28 days. Large image and zoom-in scale bars are 1 mm and 250  $\mu\text{m}$ , respectively, (b) quantification of fascicle number after encapsulation and biopreservation for indicated time, and (c) quantification of fascicle diameter after encapsulation and biopreservation for indicated time.

biopreservation. To further characterize the effects of biopreservation on construct architecture, images of TENGs were taken pre-encapsulation and after 7 or 28 days of biopreservation (Figure 3(a)). Fascicle number decreased from pre-encapsulation in both cases, but no significant differences were observed in the percent of fascicles remaining after 7 or 28 days (Figure 3(b)). After 28 days of biopreservation, however, the standard deviation in the percent of remaining fascicles increased markedly. Interestingly, TENGs biopreserved for 28 days exhibited the highest fascicle diameter, nearly achieving statistical significance from TENGs biopreserved for 7 days ( $p=0.056$ ). Again, fascicle diameter standard deviation was higher in the 28-day group than in the other conditions.

#### Biopreserved TENG protein expression in vitro

To assess potential impacts of biopreservation on neuron-specific cytoskeletal and nuclear protein expression, TENGs freshly prepared or biopreserved for 7 or 28 days were fixed and stained for  $\beta$ -III tubulin, neurofilament 200

(200 kDa), and NeuN (Figure 4(a)). Fresh or biopreserved TENGs exhibited similar staining intensities for  $\beta$ -III tubulin and neurofilament 200 (Figure 4(b) and (c)). In the 28-day group, neurofilament staining intensity trended towards higher, but this was not found to be statistically significant (Figure 4(c)).

Expression of the neuronal nuclei marker NeuN sharply decreased after 28 days of biopreservation as assessed by quantification of the area percentage of TENG DRG clusters expressing NeuN, although this failed to reach significance by the 0.05 cutoff ( $p=0.11$ ; Figure 4(d)). Importantly, this apparent decrease in NeuN+ area was not due to proliferation of non-neuronal cells, as evidenced by stable aggregate size over time (Supplemental Figure 2).

#### Biopreserved TENGs survive transplantation in vivo

From a product development perspective, the functional consequences of biopreservation are of critical importance. To characterize the impacts of biopreservation on

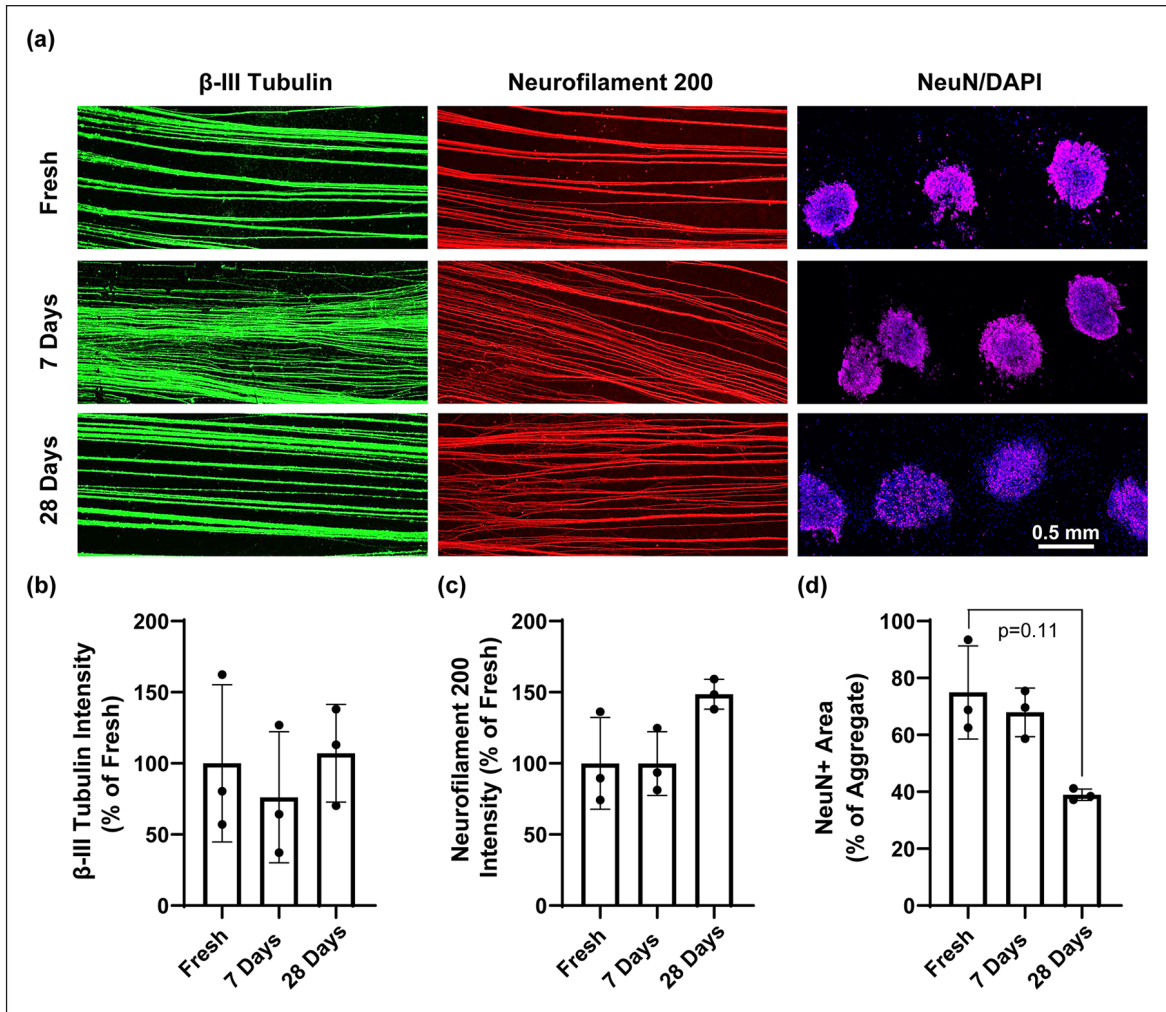


**Figure 4.** Biopreserved TENGs express typical axoskeletal proteins but may decrease neuronal nuclei (NeuN) expression with time: (a) representative images of TENGs stained with antibodies raised against  $\beta$ -III tubulin, 200 kDa neurofilament, or neuronal nuclei (NeuN), (b) quantification of  $\beta$ -III tubulin staining intensity, (c) quantification of neurofilament 200 staining intensity, and (d) quantification of area % of neuronal aggregates expressing NeuN.

product performance, fresh or biopreserved TENGs were housed in clinically available crosslinked collagen nerve wraps and sutured into 1 cm defects in the rat sciatic nerve. Animals were randomly assigned to receive fresh TENGs, 7-day biopreserved TENGs, or 28-day biopreserved TENGs. All fresh and 7-day biopreserved TENGs, as well as a subset ( $n=2$ ) of 28-day biopreserved TENGs, were transduced to express green fluorescent protein (GFP) prior to transplant. Graft regions were collected after 2 weeks *in vivo*. From longitudinal sections of the graft region, TENGs were identified by either GFP signal (in transduced TENGs) or neurofilament staining of neuronal somas (in non-transduced TENGs). After 2 weeks *in vivo*, evidence of TENG survival (DRG clusters and associated axons) could be routinely found in all groups (Figure 5(a) and (b)). Across all animals, only one transplant exhibited a complete lack of survival. The case of no survival occurred in the fresh group and was likely a consequence of accidentally damaging the delicate tissue

during encapsulation and transfer from bioreactor to nerve guidance conduit. This case was excluded from subsequent analyses.

In order to more closely investigate TENG health *in vivo*, a semi-quantitative *in vivo* TENG health/architecture score was applied in all cases of TENG survival. TENG health/architecture scores are based on a combination of TENG architecture and cellular morphology and range from 1 to 5, with five being the healthiest score (Supplemental Figure 1). While all TENGs exhibited similar average scores regardless of biopreservation status, the largest standard deviation was observed in the scores of TENGs preserved for 28 days, with two of the six animals receiving scores of 1/5 (Figure 5(c)). Individual surviving TENG DRG were also assigned a TENG DRG health score of 1–5 according to neuronal morphology, revealing little differences in fresh versus biopreserved groups (data presented in Figure 5(d); scale described in Supplemental Figure 1).



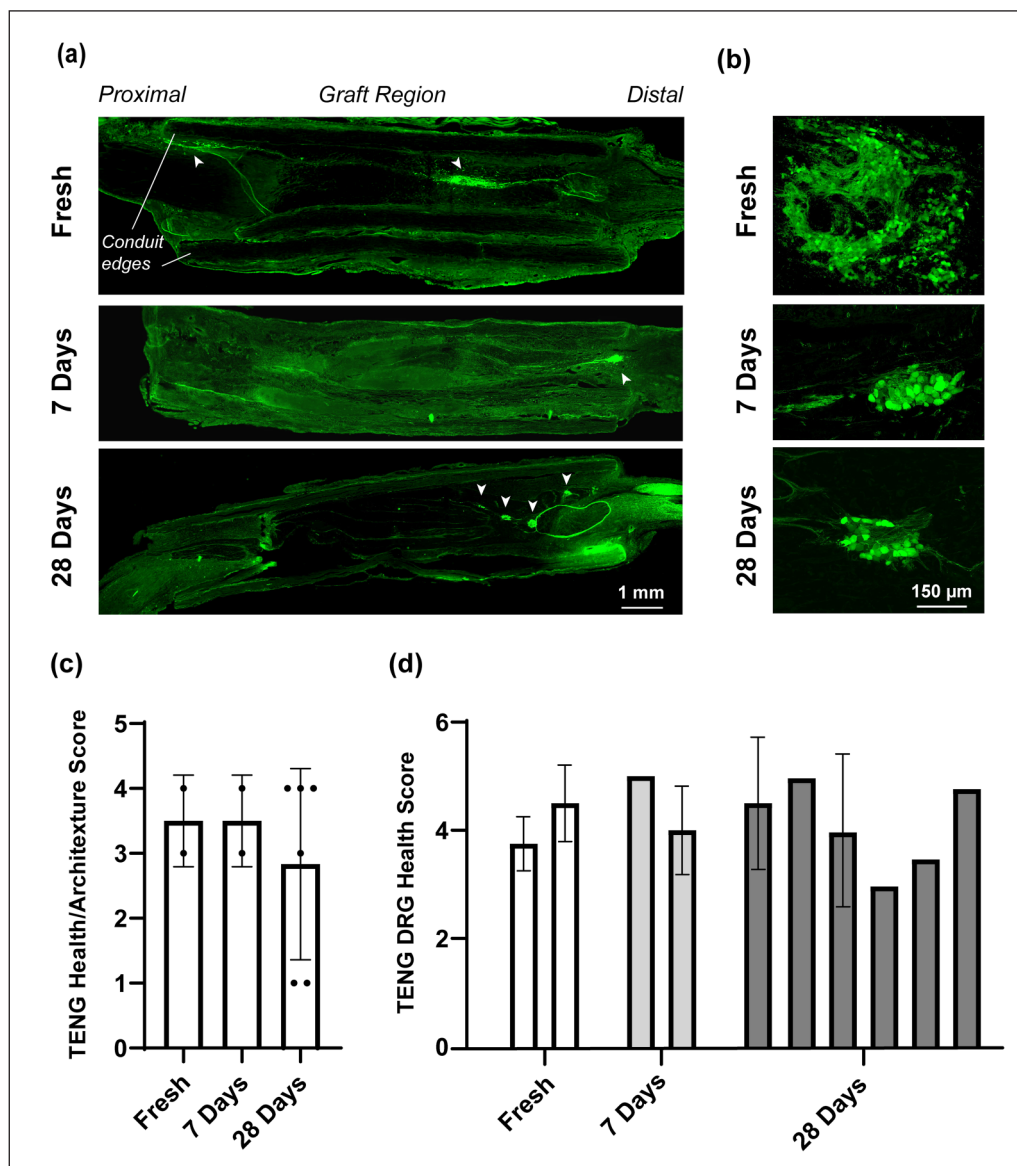


**Figure 5.** At 2 weeks post-transplant, fresh and biopreserved TENGs frequently survive: (a) longitudinal sections of graft regions (20  $\mu\text{m}$ ); arrowheads mark GFP+ TENG-derived sensory neuron clusters (DRG), (b) high magnification images of representative DRG clusters, (c) semi-quantitative TENG health/architecture scores; columns represent average score across each condition, and points represent individual animals, and (d) semi-quantitative health scores for individual TENG-derived DRG; each column represents average TENG DRG health scores for a single animal (no error bars are present when all DRG in a single animal share the same score).

### Biopreserved TENGs upregulate neurofilament expression *in vivo*

After 2 weeks *in vivo*, exogenous DRG from biopreserved TENGs exhibited increased staining intensity when labeled with a cocktail of antibodies raised against phosphorylated and nonphosphorylated NF-H (Figure 6(a)). Modulation of neurofilament phosphorylation state occurs over the lifetime of the neuron to achieve specific functions.<sup>23</sup> To identify the complete heavy-chain neurofilament axoskeleton, staining was performed with antibodies raised against both isoforms. TENG NF-H staining intensity was then normalized to host axon NF-H staining intensity at the

proximal end of the same section. TENGs from the 28-day biopreservation group exhibited significantly higher NF-H intensity as compared with fresh TENGs or TENGs biopreserved for 7 days (Figure 6(b)).

### Fresh and biopreserved TENGs interact with Schwann cells

At 2 weeks post-transplant, both fresh and biopreserved TENG neurons and axons were found to closely interact with S100+ SCs (Figure 7(a)). TENG recruitment of SCs into the graft region has been previously described and is believed to be one of several mechanisms by which TENGs





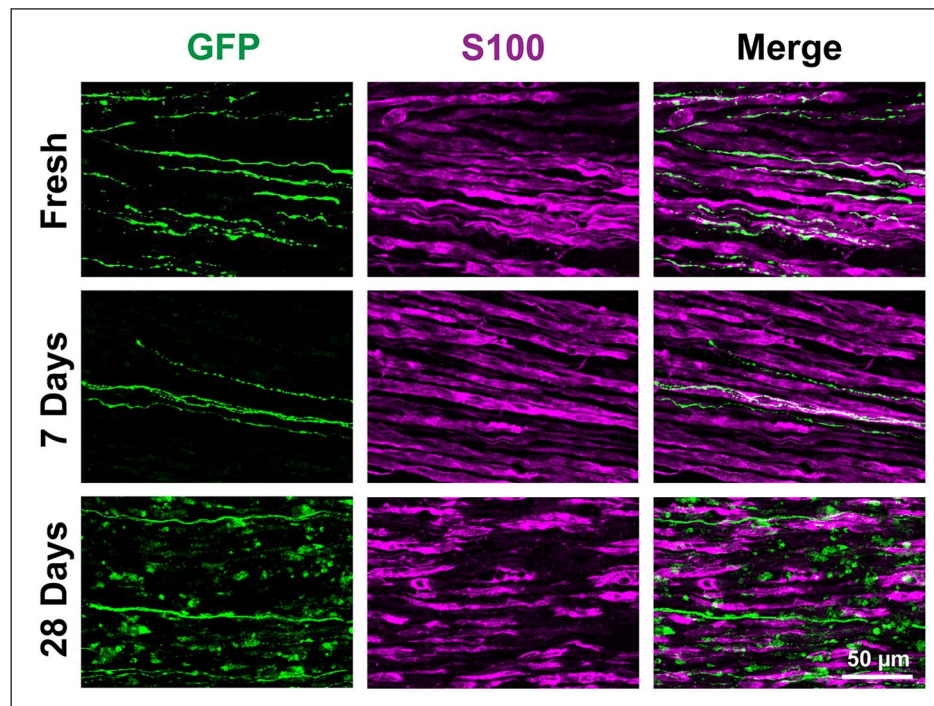


**Figure 8.** At 2 weeks post-transplant, fresh and biopreserved GFP+ TENGs extended axons along aligned host Schwann cells into proximal and/or distal nerve stumps in all groups.

(14 days), as described previously.<sup>17</sup> In this context, the regenerative front is defined as the bolus of axons emanating from the proximal end of the graft. To quantify SC infiltration, the lengths of inward migration (end of the nerve wrap to the innermost SC) was measured at both proximal and distal ends of the graft zone. The sum of the proximal and distal SC infiltration lengths was then normalized to the length of the nerve wrap and total SC infiltration was expressed as a percentage of the total wrap length. Quantification methods are illustrated in Figure 9(a). Across groups, average regeneration rates were  $0.34 \pm 0.14$ ,  $0.34 \pm 0.05$ , and  $0.27 \pm 0.03$  mm/day in fresh, 7 day, and 28 day biopreserved groups, respectively (Figure 9(b)). SC infiltration spanned  $79\% \pm 21\%$ ,  $68\% \pm 15\%$ , and  $75\% \pm 10\%$  of the length of conduits in fresh, 7 day, and 28 day biopreserved groups, respectively. At 2 weeks post-transplant, axon regeneration and SC infiltration were thus found to be relatively consistent across all repair strategies, indicating that biopreservation did not appear to impact TENG-mediated nerve regeneration.

## Discussion

Hypothermic biopreservation strategies exploit the temperature dependence of nearly all cellular functions. The activities of most enzymes are thought to decrease 1.5-2-fold for every 10°C decrease in temperature.<sup>24</sup> Accordingly, cells maintained in hypothermic environments also require far less nutrients to remain viable as energy expenditure is

significantly reduced. While hypothermia effectively slows cellular processes, it can also inflict injury upon cells. Under hypothermic conditions, temperature-dependent membrane pump activity dramatically slows, severely compromising cellular ability to maintain normal ionic gradients.<sup>25</sup> Without functioning membrane pumps, sodium and chlorine ions passively diffuse down their concentration gradients and into cells, resulting in intracellular hyperosmolarity. Water follows, causing swelling and potential lysis.<sup>24,26</sup> In addition to swelling, hypothermic cells can also experience ATP depletion, intracellular calcium accumulation, reactive oxygen species generation, and increased glycolytic production of lactic acid, plunging intracellular pH to dangerously acidic levels.<sup>2,27,28</sup> Temperature also exerts physical effects on cells as membrane lipids undergo thermotropic phase transitions from liquid to gel states, destabilizing membrane structures.<sup>29-31</sup> This stiffening of neurolemmal membranes likely explains observations of increased neuronal sensitivity to mechanical stress following refrigeration.<sup>32</sup> Successful hypothermic storage of bioengineered tissue thus hinges on the use of preservation medias carefully formulated to provide essential nutrients while also protecting cells against cold-induced insults. To date, several commercially available and clinically tested solutions have been developed including Belzer UW Cold Storage Solution (Bridge to Life Ltd.) and HypoThermosol (BioLife Solutions). Because neuronal tissues have a unique set of nutrient requirements and can be comparatively more difficult to maintain than

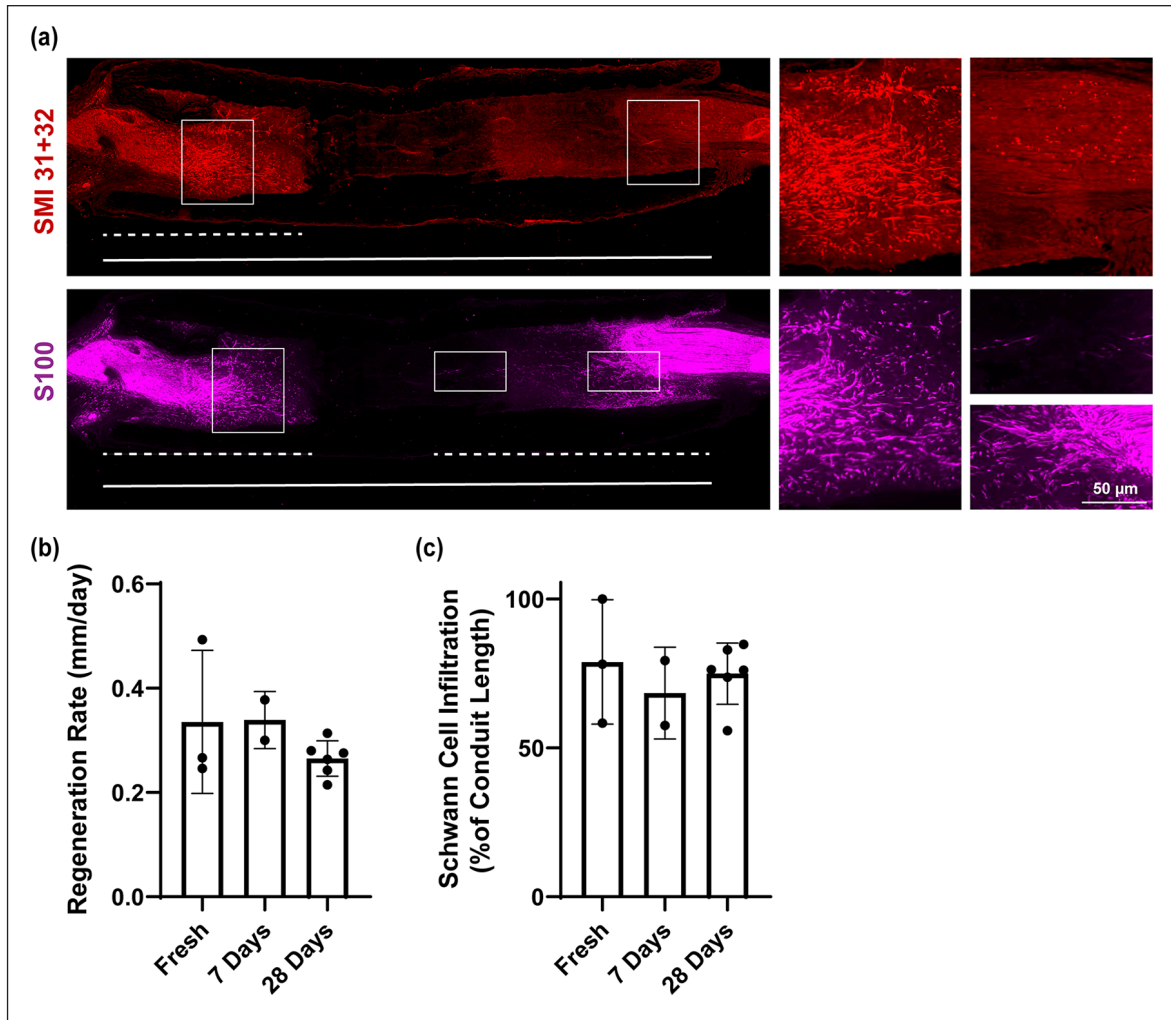


**Figure 9.** TENG biopreservation does not appear to influence regeneration at 2 weeks post-transplant: (a) examples of longitudinal sections stained for axons or Schwann cells (28 days group). Dotted lines indicate distance of axon regeneration or Schwann cell infiltration; solid lines denote conduit length, (b) quantification of axon regeneration rate (regenerative front distance in mm/14 days), and (c) quantification of Schwann cell infiltration (proximal + distal, normalized to conduit length).

other cell types, we chose to use Hibernate-E (ThermoFisher Scientific), a cold storage media designed for the preservation of embryonic rodent brain tissue when supplemented with B27 and Glutamax.

Post-preservation, TEMP built from living cells must remain viable and retain sufficient bioactivity/potency to achieve therapeutic benefit in patients. Despite increasing interest in commercialization of tissue engineered medical products, only a handful of studies describe the development of TEMP biopreservation strategies. These include hypothermic and cryogenic storage of tissue engineered bone (48 h at 4 or  $-80^{\circ}\text{C}$ ), synthetic human epidermis (up to 13 days at  $4^{\circ}\text{C}$ ), articular cartilage (up to 56 days at room temperature, 4 or  $37^{\circ}\text{C}$ ), human adipose stem cell sheets (3 or 7 days at  $4^{\circ}\text{C}$ ), and aligned SC columns in a collagen matrix (2 days at  $4^{\circ}\text{C}$  or 1 day at  $-80^{\circ}\text{C}$  followed by 2 days in liquid nitrogen).<sup>6,8,11,33,34</sup> These studies exclusively

employ *in vitro* assays to evaluate viability and potency. Tissue engineered bone maintained viability and extracellular matrix integrity following refrigeration but not freezing.<sup>11</sup> Synthetic epidermis remained viable for up to 9 days of refrigeration.<sup>8</sup> Articular cartilage maintained viability, glycosaminoglycan content and collagen content for 28 days at both room temperature and  $4^{\circ}\text{C}$  (at least partly due to the low metabolic demands of chondrocytes native to avascular tissue beds *in vivo*).<sup>33</sup> Lastly, SCs survived and promoted DRG neurite outgrowth *in vitro* following 2 days at  $4^{\circ}\text{C}$ .<sup>34</sup> Notably, this study was performed in Hibernate-A, another neural-specific hibernation media developed for adult tissue preservation. Some SC survival and guidance of neurites *in vitro* were also observed after 3 days under frozen conditions. By contrast, to study the effect of cold storage on our constructs, biopreserved TENGs were assessed using both *in vitro* and *in vivo*



methods. While *in vitro* assays provide an important description of biopreserved TEMPs pre-transplantation, these measures only offer predictions of TEMP potency. Some of these *in vitro* descriptors can ultimately serve as quality control and assurance measures, but *in vivo* performance is the most important outcome measure for evaluating TEMP biopreservation strategies.

TENGs were found to survive biopreservation for up to 4 weeks, although overall construct health declined with increasing preservation time as evidenced by increased LDH enzyme release as well as a trend towards reduced expression of NeuN, a phenomenon often associated with neuronal stress or degeneration.<sup>19,21,35</sup> Similar findings were noted *in vivo*; after transplantation for 2 weeks, biopreserved TENGs were again found to routinely survive, but with an apparent increase in health score standard deviation following 28 days of biopreservation as compared with 7-day and fresh TENGs.

Our data also suggest that TENGs undergo progressive maturation throughout the preservation process. Some maturation is to be expected since cells remain metabolically active (albeit at greatly reduced rates) under refrigeration; suspended animation, the true biological “pause button,” is not achieved until deep subzero temperatures are reached. Characterization of fascicular architecture of biopreserved TENGs revealed a potential trend towards increased fascicle diameter with increasing biopreservation time. This trend could indicate an increase in individual axon diameter or increased fascicular bundling, both of which are indicative of tissue maturation. Fascicular bundling would be expected to result in a decrease in fascicle number, but the high variability in the 28-day group makes it difficult to support this conclusion. Even more compelling evidence of maturation was found *in vivo*, where 28-day biopreserved TENGs exhibited significantly brighter neurofilament staining intensities as compared with fresh and 7-day controls. In cultured neurons, NF-H expression is associated with maturation<sup>23</sup> Accordingly, increased expression of heavy neurofilament species throughout biopreservation could be interpreted as neuronal maturation. A similar (but not statistically significant) trend was also observed from *in vitro* characterization of biopreserved TENG neurofilament expression, suggesting extended biopreservation may provide a maturation “head start” that proceeds following transplantation. Finally, biopreservation time (up to 4 weeks) did not strongly predict TENG function *in vivo*. Instead, fresh and biopreserved TENGs were frequently found to robustly interact with S100+ SCs and extend neurites into distal nerve segments, two important mechanisms by which TENGs are believed to augment the regenerative response to PNI and promote functional recovery.<sup>17</sup> Indeed, nerves repaired with fresh or biopreserved TENGs exhibited similar degrees of host axon regeneration and SC infiltration, suggesting that biopreservation for up to 4 weeks does not

negatively influence TENG-mediated nerve regeneration. Collectively, our data suggest that biopreservation modulates TENG health and maturity, but is not a strong predictor of TENG survival, health, and function *in vivo* as similar pro-regenerative metrics were achieved between fresh and preserved TENGs. Notably, however, our findings suggest that extended biopreservation times are likely to introduce variability in construct behavior, resulting in a less consistent product.

Despite the high energetic needs of neurons with centimeter-scale axons, long-term hypothermic biopreservation was achieved. This was likely possible due to the combination of nutrient-rich media and reduced metabolic needs under refrigeration. In addition, because TENG cultures are encapsulated in thin collagen sheets, mass transport of solutes including oxygen and waste can readily occur via simple diffusion. Ultimately, clinical TENG products will be built from GalSafe<sup>®</sup> neurons, which are genetically modified porcine cells that have been engineered to elicit minimal to no immune responses following human implantation. Manufacturing of TENGs from this biomass has already been demonstrated by our group.<sup>15</sup> Based on our findings, the storage strategy illustrated here is also expected to preserve TENGs built from porcine GalSafe<sup>®</sup> neurons. This encouraging work thus motivates ongoing investigations of chronic efficacy of biopreserved TENGs built from translationally-viable biomass for the repair of critical nerve defects in both rodent and large animal models. These studies will also include an investigation of potential chronic inflammatory responses following biopreserved TENG implantation to ensure that any biopreservation-induced degeneration of the TENG does not result in an excessive inflammatory response. Lastly, identification of key nondestructive *in vitro* metrics that strongly correlate with *in vivo* success is also required to establish release criteria for the final clinical product.

## Conclusion

Collectively, the data discussed here demonstrate for the first time the feasibility of preserving TENGs for up to a month at 4°C. To our knowledge, this marks the first attempt to biopreserve any tissue engineered neuron-based construct. Through this study, we established a simple cold storage protocol and biopreservation timeframe guidelines of interest to the neural tissue engineering community at large. Notably, variability in some *in vitro* and *in vivo* outcome measures increased dramatically after 28 days of biopreservation as compared with fresh or 7-day biopreserved TENGs, suggesting a more consistent product may be obtained if biopreservation time is limited to less than 4 weeks or biomanufacturing and preservation protocols are further refined. This work also represents several major milestones in TENG product development as establishment of shelf-life can address multiple logistical hurdles



that would otherwise prevent widespread clinical usage. These studies motivate future work to establish quality control, quality assurance, and release criteria for clinical TENG products, as well as execution of IND-enabling safety and efficacy studies investigating biopreserved TENGs in appropriate preclinical models of major PNI repair.

### Data Availability

All data is available upon request.

### Declaration of conflicting interests

The author(s) declared the following potential conflicts of interest with respect to the research, authorship, and/or publication of this article: D.K.C. is a co-founder and K.S.K. and R.B.S. are employees of Axonova Medical, LLC, which is a University of Pennsylvania spin-out company focused on translation of advanced regenerative therapies to treat nervous system disorders. Multiple patents related to the composition, methods, and use of tissue engineered nerve grafts, including U.S. Patent 9,895,399 (D.K.C.), US Patent 10,525,085 (D.K.C.), U.S. Patent App. 16/753,634; (D.K.C.), and U.S. Provisional Patent App. 62/937,489 (D.K.C & J.C.B.). No other author has declared a potential conflict of interest.

### Funding

The author(s) disclosed receipt of the following financial support for the research, authorship, and/or publication of this article: Financial support provided by the National Institutes of Health [NINDS R44-NS108869 (Katiyar & Cullen) & NIBIB T32-EB005583 (Shultz)], the U.S. Department of Defense [CDMRP/JPC8-CRMRP W81XWH-16-1-0796 (Cullen) & CDMRP/PRORP W81XWH-19-1-0867 (Cullen)], the Department of Veterans Affairs [BLR&D Merit Review I01-BX003748 (Cullen)], and the Advanced Regenerative Manufacturing Institute [ARMI-T0080 (Katiyar & Cullen)]. Opinions, interpretations, conclusions and recommendations are those of the author(s) and are not necessarily endorsed by the National Institutes of Health, the Department of Defense, the Department of Veterans Affairs, or the Advanced Regenerative Manufacturing Institute.

### ORCID iD

Robert B Shultz  <https://orcid.org/0000-0002-2424-5972>

### Supplemental material

Supplemental material for this article is available online.

### References

1. Giwa S, Lewis JK, Alvarez L, et al. The promise of organ and tissue preservation to transform medicine. *Nat Biotechnol* 2017; 35: 530–542.
2. Acker JP. Biopreservation of cells and engineered tissues. *Adv Biochem Eng Biotechnol* 2007; 103: 157–187.
3. Högman CF. Liquid-stored red blood cells for transfusion. A status report. *Vox Sang* 1999; 76: 67–77.
4. Ostrowska A, Gu K, Bode DC, et al. Hypothermic storage of isolated human hepatocytes: a comparison between University of Wisconsin solution and a hypothermosol platform. *Arch Toxicol* 2009; 83: 493–502.
5. Petrenko Y, Chudickova M, Vackova I, et al. Clinically relevant solution for the hypothermic storage and transportation of human multipotent mesenchymal stromal cells. *Stem Cells Int* 2019; 2019: 5909524.
6. Freitas-Ribeiro S, Carvalho AF, Costa M, et al. Strategies for the hypothermic preservation of cell sheets of human adipose stem cells. *PLoS One* 2019; 14: e0222597.
7. Armitage WJ. Preservation of human cornea. *Transfus Med Hemother* 2011; 38: 143–147.
8. Cook JR, Eichelberger H, Robert S, et al. Cold-storage of synthetic human epidermis in hypothermosol. *Tissue Eng* 1995; 1: 361–377.
9. DeBono R, Rao GS and Berry RB. The survival of human skin stored by refrigeration at 4 degrees C in McCoy's 5A medium: does oxygenation of the medium improve storage time? *Plast Reconstr Surg* 1998; 102: 78–83.
10. Evans PJ, MacKinnon SE, Midha R, et al. Regeneration across cold preserved peripheral nerve allografts. *Microsurgery* 1999; 19: 115–127.
11. Tam E, McGrath M, Sladkova M, et al. Hypothermic and cryogenic preservation of tissue-engineered human bone. *Ann N Y Acad Sci* 2020; 1460: 77–87.
12. Jing L, Yao L, Zhao M, et al. Organ preservation: from the past to the future. *Acta Pharmacol Sin* 2018; 39: 845–857. 2018/03/23.
13. Gillooly JF, Brown JH, West GB, et al. Effects of size and temperature on metabolic rate. *Science* 2001; 293: 2248–2251.
14. Pfister BJ, Gordon T, Loverde JR, et al. Biomedical engineering strategies for peripheral nerve repair: surgical applications, state of the art, and future challenges. *Crit Rev Biomed Eng* 2011; 39: 81–124.
15. Katiyar K, Burrell JC, Laimo F, et al. Biomanufacturing of axon-based tissue engineered nerve grafts using porcine GalSafe<sup>®</sup> neurons. *Tissue Eng Part A*. Epub ahead of print 9 April 2021. DOI: 10.1089/ten.TEA.2020.0303.
16. Pfister BJ, Iwata A, Meaney DF, et al. Extreme stretch growth of integrated axons. *J Neurosci* 2004; 24: 7978–7983.
17. Katiyar KS, Struzyna LA, Morand JP, et al. Tissue engineered axon tracts serve as living scaffolds to accelerate axonal regeneration and functional recovery following peripheral nerve injury in rats. *Front Bioeng Biotechnol* 2020; 8: 492.
18. Huang JH, Cullen DK, Browne KD, et al. Long-term survival and integration of transplanted engineered nervous tissue constructs promotes peripheral nerve regeneration. *Tissue Eng Part A* 2009; 15: 1677–1685.
19. Maggiore JC, Burrell JC, Browne KD, et al. Tissue engineered axon-based “living scaffolds” promote survival of spinal cord motor neurons following peripheral nerve repair. *J Tissue Eng Regen Med* 2020; 14(12): 1892–1907.
20. Cullen DK, Ezra M, Brown K, et al. Tissue engineered nerve grafts with aligned axonal tracts facilitate regeneration across 5 cm peripheral nerve lesions in swine. In: *2015 ASPN Annual Meeting*, Paradise Island, Bahamas, 2014, p.S40. Beverly MA: American Society for Peripheral Nerve.

21. Keating CE, Browne KD, Duda JE, et al. Neurons in sub-cortical oculomotor regions are vulnerable to plasma membrane damage after repetitive diffuse traumatic brain injury in swine. *J Neurotrauma* 2020; 37: 1918–1932.
22. Panzer KV, Burrell JC, Helm KVT, et al. Tissue engineered bands of büngner for accelerated motor and sensory axonal outgrowth. *Front Bioeng Biotechnol* 2020; 8: 580654.
23. Pant HC and Veeranna. Neurofilament phosphorylation. *Biochem Cell Biol* 1995; 73: 575–592.
24. Belzer FO and Southard JH. Principles of solid-organ preservation by cold storage. *Transplantation* 1988; 45: 673–676.
25. Honig A, Oppermann H, Budweg C, et al. Demonstration of temperature dependence of Na(+)-K+ pump activity of human blood cells. *Am J Physiol* 1994; 266: S10–S15.
26. Petrowsky H and Clavien P-A. Chapter 44 - Principles of liver preservation. In: Busuttil RW and Klintmalm GBG (eds) *Transplantation of the liver*. 3rd ed. Philadelphia, PA: W.B. Saunders, 2015, pp.582–599.
27. Brinkkoetter PT, Song H, Lösel R, et al. Hypothermic injury: the mitochondrial calcium, ATP and ROS love-hate triangle out of balance. *Cell Physiol Biochem* 2008; 22: 195–204.
28. Rauen U and de Groot H. Mammalian cell injury induced by hypothermia- the emerging role for reactive oxygen species. *Biol Chem* 2002; 383: 477–488.
29. Drobnis EZ, Crowe LM, Berger T, et al. Cold shock damage is due to lipid phase transitions in cell membranes: a demonstration using sperm as a model. *J Exp Zool* 1993; 265: 432–437.
30. Watson PF and Morris GJ. Cold shock injury in animal cells. *Symp Soc Exp Biol* 1987; 41: 311–340.
31. Tsvetkova NM, Crowe JH, Walker NJ, et al. Physical properties of membrane fractions isolated from human platelets: implications for chilling induced platelet activation. *Mol Membr Biol* 1999; 16: 265–272.
32. Kawamoto JC and Barrett JN. Cryopreservation of primary neurons for tissue culture. *Brain Res* 1986; 384: 84–93.
33. Nover AB, Stefani RM, Lee SL, et al. Long-term storage and preservation of tissue engineered articular cartilage. *J Orthop Res* 2016; 34: 141–148.
34. Day AGE, Bhangra KS, Murray-Dunning C, et al. The effect of hypothermic and cryogenic preservation on engineered neural tissue. *Tissue Eng Part C Methods* 2017; 23: 575–582.
35. Wu K-L, Li Y-Q, Tabassum A, et al. Loss of neuronal protein expression in mouse hippocampus after irradiation. *J Neuropathol Exp Neurol* 2010; 69: 272–280.